SOLVING FOURTH-ORDER PARTIAL DIFFERENTIAL EQUATIONS USING RADIAL BASIS FUNCTION COLLOCATION METHODS

B. KHATRI GHIMIRE[1], A. R. LAMICHHANE[2‡], D. WATSON[3], AND Z. ZHOU[4]

[1]Department of Mathematics and Computer Science, Alabama State University,
Montgomery, Alabama 36104, USA
[2]Department of Mathematics and Statistics, Ohio Northern University
Ada, Ohio 45810, USA
[3]Department of Mathematics, University of Southern Mississippi
Hattiesburg, Mississippi 39406, USA
[4]School of Computing, University of Southern Mississippi
Hattiesburg, Mississippi 39406, USA

ABSTRACT. In this paper, we propose a new approach for solving fourth-order partial differential equations (PDEs) which uses an intermediate step so that fourth order PDEs can be reduced to second order PDEs. This method is simple and easy to implement. We compare the numerical result of this method to the Kansa method and the method of approximate particular solutions (MAPS). We also observe the numerical accuracy of the proposed method on the local Kansa method (LKM) and localized method of approximate particular solutions (LMAPS). Numerical results show that this method outperforms the MAPS and Kansa method in both global and local cases.

AMS (MOS) Subject Classification. 65N35.

1. INTRODUCTION

During the past quarter century, radial basis functions (RBFs) have played an important role in state-of-the-art meshless methods for solving partial differential equations (PDEs). In general, there are three main considerations for solving PDEs - accuracy, efficiency and simplicity. To fulfill these criteria, Edward Kansa [7] developed the radial basis function collocation method (RBFCM) which is known as the Kansa method. The Kansa method has been successfully applied to solve many challenging problems in science and engineering. Followed by several developments of meshless methods Chen *et al.* [2] proposed a new method called the method of approximate particular solutions (MAPS) which uses the particular solution of RBFs to approximate the differential equation. The main disadvantages of the RBF collocation method are related to the formation of full and dense matrices that are very

‡Corresponding author

sensitive to the choice of the free shape parameter and the difficulty in solving problems with a large number of unknowns. This is due to the use of the radial basis function interpolation which increases the condition numbers of the related matrices as the number of nodes increases. Various kinds of RBF collocation methods have been developed to overcome the difficulties of full, dense, and ill-conditioned matrices arising from the early version of the RBF collocation method. To mitigate the computational cost for large-scale problems, Mai-Duy *et al.* [11] employed the domain decomposition method. In 2002, Chen *et al.* [3] proposed a multi-grid approach using compactly supported RBFs. In recent years, the localized version of RBF collocation methods such as the local Kansa method (LKM) and the localized method of approximate particular solutions (LMAPS) [15, 18] have been developed and widely used for solving large-scale problems. The main advantage of the local version of the RBF collocation methods is the collocation on subdomains which drastically reduces the collocation matrix size. These new methods have been proven as effective numerical methods to alleviate the problems of dense and ill-conditioned matrices. The latest development of RBF collocation methods has grown to compete with the traditional mesh-based numerical methods, such as finite element and finite difference methods. We have seen extensive research in industrial applications, science, and engineering which shows that RBF collocation methods are maturing and becoming accepted as a method of choice for solving PDEs by researchers and practitioners.

Fourth order partial differential equations (PDEs) have a wide range of applications in various fields of science and engineering. Some examples of physical flows and engineering problems modeled by fourth order PDEs are ice formation [13], fluids on lungs [6], image processing for noise removal [8, 10], etc. Yao *et al.* [19] compared three meshless methods- LMAPS, local direct RBF collocation method (LDRBFCM), and local indirect RBF collocation method (LIRBFCM)- for solving heat diffusion equations. In [19], authors concluded that LMAPS and LIRBFCM had slightly better results. In this paper, we focus on RBF collocation methods for solving fourth-order PDEs in both global and local cases. First, we use the Kansa method and the method of approximate particular solutions using multiquadric (MQ) and normalized multiquadric (NMQ) radial basis functions. Here we note that the corresponding differentiations and integrations are required to obtain closed form particular solutions of RBFs. Next, we employ the new approach for solving fourth-order PDEs both locally and globally. Finally, direct RBFCMs and new RBFCMs are compared for the approximation of functions.

The organization of this paper is as follows. In section 2, the type of PDEs with various kinds of boundary conditions is listed. In section 3, we briefly introduce some RBF collocation methods: Kansa method, method of approximate particular solutions (MAPS) and localized method of approximate particular solutions (LMAPS).

The formulation of the new approach is briefly explained in section 4. In section 5, we present the numerical results and we draw conclusions from the comparisons in section 6.

2. GOVERNING EQUATIONS

Let us limit our discussion to the solution of fourth-order PDEs defined on a fixed domain Ω with boundary $\partial\Omega$ in 2D,

$$(2.1) \qquad Lu(x,y) = f(x,y), \quad (x,y) \in \Omega,$$

Dirichlet boundary condition

$$(2.2) \qquad u(x,y) = g(x,y), \quad (x,y) \in \partial\Omega,$$

Neumann boundary condition

$$(2.3) \qquad \frac{\partial u(x,y)}{\partial \mathbf{n}} = h(x,y), \quad (x,y) \in \partial\Omega,$$

where

$$L = \Delta^2 + \alpha(x,y)\frac{\partial}{\partial x} + \beta(x,y)\frac{\partial}{\partial y} + \gamma(x,y),$$

Δ^2 denotes the biharmonic operator, Δ denotes the Laplace operator, $\partial/\partial\mathbf{n}$ is the normal derivatives on the boundary $\partial\Omega$, and α, β, γ, f, g, h are given functions.

3. RBF COLLOCATION METHODS

3.1. **Kansa Method.** The Kansa method [7], pioneered by Edward Kansa in 1990, is considered to be the first RBF collocation method. This method has been successfully applied to solve linear and non-linear PDEs. The only geometric property utilized in this method is the distance between points in the computational domain; consequently, extending to a higher dimension does not increase the difficulty of the method. To briefly explain the Kansa method, we consider the following simple boundary value problem:

$$(3.1) \qquad \begin{aligned} \mathcal{L}u(x) &= f(x), \quad x \in \Omega, \\ \mathcal{B}u(x) &= g(x), \quad x \in \partial\Omega, \end{aligned}$$

where $\mathcal{L}$ is a differential operator, $\mathcal{B}$ is a boundary differential operator, f and g are known functions, Ω is a domain, and $\partial\Omega$ is the boundary of Ω. The important part of the Kansa method involves approximating the solution u with a linear combination of RBFs, i.e.,

$$\hat{u}(x) = \sum_{j=1}^{N} \alpha_j \phi(\|x - x_j\|),$$

where $\{\alpha_j\}_{j=1}^N$ are undetermined coefficients. Applying the operators and utilizing the collocation techniques yield

$$(3.2) \qquad \sum_{j=1}^N \alpha_j \mathcal{L}\phi(\|x_k - x_j\|) = f(x_k), \quad k = 1, 2, \ldots, N_i,$$

and

$$(3.3) \qquad \sum_{j=1}^N \alpha_j \mathcal{B}\phi(\|x_k - x_j\|) = g(x_k), \quad k = N_i + 1, \ldots, N,$$

where N_i denotes the number of interior points and the number of boundary nodes is denoted by N_b, i.e., $N = N_i + N_b$. The system (3.2) and (3.3) is a square linear system for which $\{\alpha_j\}_{j=1}^N$ can be obtained using any appropriate linear system solver.

3.2. **Method of Approximate Particular Solutions.** Chen *et al.* [2] proposed the method of approximate particular solutions (MAPS) to improve the method of particular solutions (MPS) by avoiding the calculation of the homogeneous solution. Using the RBFs, an approximate particular solution to (3.1) is given by

$$\hat{u}(x) = \sum_{i=1}^N \alpha_i \Phi(r_i).$$

Here we note that

$$\mathcal{L}\Phi(r) = \phi(r),$$

where $\mathcal{L}$ is a differential operator and $\Phi(r)$ is the particular solution for the corresponding RBF $\phi(r)$. It is worth noting that the MAPS representation appears similar to the Kansa method. The major distinction between MAPS and Kansa method is that the MAPS derives the corresponding particular solution Φ by a reverse differentiation process. Thus, the MAPS may have a more sound mathematical foundation.

3.3. **Localized Method of Approximate Particular Solutions.** Different from the global methodologies and inspired by the idea of CS-RBFs, a number of localized methods have been proposed to alleviate the ill-conditioning of the resultant matrix, the costly dense matrix of the RBF interpolation, and the uncertainty of the selection of the optimal shape parameter. Instead of solving a dense matrix in the global approach, the local approach results in a sparse matrix that can be solved efficiently [18].

Let $\{x_i\}_{i=1}^N$ be a set of collocation points in $\Omega \cup \partial\Omega$. For each $x_i \in \Omega$ we choose the nearest neighbor points $\Omega_i = \{x_k^i\}_{k=1}^n$, where $x_k^i = x_{k(i)}$ denotes the local indexing for each collocation point belonging to Ω_i. The construction requires that $\Omega_i \cap \Omega_j \neq \phi$ for some $j \neq i$ and $\{x_i\}_{i=1}^N = \cup_i \Omega_i$. Our purpose is to formulate a numerical scheme to approximate $u(x)$ and its derivatives at all collocation points x_i. Since these points

can be selected arbitrarily in the domain, we can always choose the points where the approximate solutions are needed as the collocation points.

Consider the collocation method on the local domain Ω_i and let $x_i = x_k^i \in \Omega_i$ for some $k \leq n$. Then $u(x_i)$ can be approximated by a localized formulation as follows:

$$(3.4) \qquad \hat{u}(x_i) = \sum_{k=1}^{n} \alpha_k^i \Phi(\|x_i - x_k^i\|),$$

where n is the number of the nearest neighboring points x_k^i surrounding collocation point x_i, including the collocation point itself, α_k^i are the unknown coefficients to be determined, and $\Phi(x)$ is an RBF. It can be proved that Φ is non-singular such that the inverse matrix can always be computed provided that all the nodal points inside Ω_i are distinct points. The unknown coefficients can be written as follows:

$$\alpha^i = \Phi^{-1}\hat{u}^i,$$

where

$$\alpha = [\alpha_1, \alpha_2, \ldots, \alpha_n]^T, \hat{u} = [\hat{u}(x_1^i), \ldots, \hat{u}(x_n^i)]^T.$$

Hence, $\hat{u}(x_i)$ can be expressed in terms of the function values at n nodal points, $\hat{u}_n$, i.e.

$$\hat{u}(x_i) = \sum_{k=1}^{n} \alpha_k \Phi(\|x_i - x_k^i\|) = \hat{\Phi}(x_i)\alpha = \hat{\Phi}(x_i)\Phi_n^{-1}\hat{u}_n,$$

$$\hat{u}(x_i) = \Psi_n(x_i)\hat{u}_n,$$

where

$$\hat{\Phi}(x_i) = [\Phi(\|x_i - x_1^i\|), \Phi(\|x_i - x_2^i\|), \ldots, \Phi(\|x_i - x_n^i\|)],$$

and

$$\Psi_n(x_i) = \hat{\Phi}(x_i)\Phi_n^{-1} = [\psi_1, \psi_2, \ldots, \psi_n].$$

Let $\hat{u}_N = [\hat{u}(x_1), \ldots, \hat{u}(x_N)]^T$. We reformulate in terms of global $\hat{u}_N$ instead of local $\hat{u}_n$ by padding the vector $\Psi_n(x_i)$ with zero entries based on the mapping between $\hat{u}_n$ and $\hat{u}_N$. It follows that

$$\hat{u}(x_i) = \Psi(x_i)\hat{u},$$

where $\Psi(x_i)$ is a $N \times N$ sparse matrix only having $N \times n$ non zero elements. Substituting in (3.4) results in a linear sparse system of equations which when solved, we get an approximate solution $\hat{u}$ at all of the collocation points.

4. **NEW FORMULATION OF FOURTH-ORDER PDEs**

The numerical approximation of higher order PDEs can be more complicated than lower orders. By reducing the order of the governing equation, we can alleviate some necessary mathematical computations in the numerical simulation. Hence, in this approach, we reduce the fourth order PDEs into two second-order PDEs. The formulation of the problem starts with the representation of $\Delta u = w$, then (2.1)–(2.3) will be reduced to the following system of equations:

$$(4.1) \qquad \Delta w(x,y) + \mathcal{L}u(x,y) = f(x,y), \quad (x,y) \in \Omega,$$

$$(4.2) \qquad w - \Delta u = 0, \quad (x,y) \in \Omega,$$

where

$$\mathcal{L} = \alpha(x,y)\frac{\partial}{\partial x} + \beta(x,y)\frac{\partial}{\partial y} + \gamma(x,y),$$

Dirichlet boundary condition

$$(4.3) \qquad u(x,y) = g(x,y), \quad (x,y) \in \partial\Omega,$$

Neumann boundary condition

$$(4.4) \qquad \frac{\partial u(x,y)}{\partial \mathbf{n}} = h(x,y), \quad (x,y) \in \partial\Omega,$$

where u, g, and h are known.

The important part of this formulation involves the approximation of the solutions u and w with a linear combination of RBFs as shown below:

$$\hat{u}(x) = \sum_{i=1}^{N} a_i \psi(\|x - x_i\|),$$

$$\hat{w}(x) = \sum_{i=1}^{N} b_i \psi(\|x - x_i\|),$$

where $\{a_i\}_{i=1}^{N}$ and $\{b_i\}_{i=1}^{N}$ are coefficients to be determined, ψ is a radial basis function and $\Delta\psi = \phi$. The above solutions u and w can be written as $\hat{u} = [\psi][a]$ and $\hat{w} = [\psi][b]$ which lead to $[a] = [\psi]^{-1}\hat{u}$ and $[b] = [\psi]^{-1}\hat{w}$. So then, (4.1)-(4.4) reduce respectively to the following equations:

$$\left[\alpha(x,y)\left[\frac{\partial\psi}{\partial x}\right][\psi^{-1}] + \beta(x,y)\left[\frac{\partial\psi}{\partial y}\right][\psi^{-1}] + \gamma(x,y)\right]\hat{u} + [\phi][\psi^{-1}]\hat{w} = f(x,y),$$

$$[\phi][\psi^{-1}]\hat{u} - \hat{w} = 0,$$

$$\hat{u} = g(x,y),$$

$$\left[\frac{\partial\psi}{\partial x}\right][\psi^{-1}]n_x + \left[\frac{\partial\psi}{\partial y}\right][\psi^{-1}]n_y = h(x,y).$$

Finally, we solve the above block matrix system to determine the unknown coefficients $\{a_i\}$ and $\{b_i\}$. Here we observe that the size of this block matrix will be twice that of the direct RBF collocation method.

4.1. **RBFs and the Particular Solutions.** In this paper, the types of radial basis functions can be chosen as needed, but the corresponding differentiations and integrations are required for the closed-form particular solutions of RBFs in both global and local cases of Kansa method and MAPS. During the past two decades, significant progress has been made in deriving closed-form particular solutions using various radial basis functions [5, 9, 12, 16]. In this paper, we used multiquadric and the normalized multiquadric (NMQ) radial basis functions for the numerical experiment. Here we list the closed-form particular solution of the normalized multiquadric in 2-D:

$$\psi(r) = \sqrt{\epsilon^2 r^2 + 1}$$

For the Kansa method, the derivation of the particular solution for the Laplacian is given by

$$\Delta\psi(r) = \frac{\epsilon^2(\epsilon^2 r^2 + 2)}{(\epsilon^2 r^2 + 1)^{\frac{3}{2}}}.$$

For the direct RBF collocation method, by direct differentiation we have,

$$\Delta^2\psi(r) = \frac{\epsilon^4(\epsilon^4 r^4 + 8\epsilon^2 r^2 - 8)}{(\epsilon^2 r^2 + 1)^{\frac{7}{2}}}.$$

For the Neumann B.C., we have

$$\frac{1}{r}\frac{\partial\psi}{\partial r} = \frac{\epsilon^2}{\sqrt{1 + (\epsilon r)^2}}.$$

For the method of approximate particular solutions (MAPS), the derivation of particular solutions for the Laplacian by inverse differentiation is given by [12]

$$\phi = \frac{1}{9}r^2\sqrt{1 + \epsilon^2 r^2} + \frac{4}{9\epsilon^2}\sqrt{1 + \epsilon^2 r^2} - \frac{1}{3\epsilon^2}\log(\sqrt{1 + \epsilon^2 r^2} + 1).$$

For the Neumann B.C., we have

$$\frac{1}{r}\frac{\partial\phi}{\partial r} = \frac{2\sqrt{1 + \epsilon^2 r^2} + \epsilon^2 r^2(\sqrt{1 + \epsilon^2 r^2} + 1) + 1}{3(\epsilon^2 r^2 + \sqrt{1 + \epsilon^2 r^2} + 1)}.$$

For the Biharmonic operator [12],

$$\begin{aligned}
\phi = {} & \frac{4r^2}{75\epsilon^2}\sqrt{1 + \epsilon^2 r^2} + \frac{r^2}{12\epsilon^2} - \frac{61}{900\epsilon^4}\sqrt{1 + \epsilon^2 r^2} \\
& - \frac{r^2}{12\epsilon^2}\log(\sqrt{1 + \epsilon^2 r^2} + 1) + \frac{r^4}{225}\sqrt{1 + \epsilon^2 r^2} + \frac{\log(\sqrt{1 + \epsilon^2 r^2} + 1)}{30\epsilon^4}.
\end{aligned}$$

For the Neumann B.C., we have

$$\frac{1}{r}\frac{\partial \phi}{\partial r} = \frac{11}{90\epsilon^2}\sqrt{1+\epsilon^2 r^2} - \frac{2\log(\sqrt{1+\epsilon^2 r^2}+1)-1}{12\epsilon^2}$$
$$+ \frac{17r^2}{450\sqrt{1+\epsilon^2 r^2}} + \frac{10\epsilon^2 r^4 + \frac{15}{\epsilon^2(\sqrt{1+\epsilon^2 r^2}+1)} + 8r^2}{450\sqrt{1+\epsilon^2 r^2}}.$$

5. NUMERICAL RESULTS

To verify the effectiveness of the new approach for solving fourth order PDEs, two numerical examples are presented. We have compared the results in terms of accuracy implementing the Kansa method directly and with the new formulation employed in this paper both globally and locally. The multiquadric (MQ) is used as a basis function. The normalized form of MQ, which is called normalized multiquadric (NMQ) has also been used as a basis function. We have also compared the errors of MQ with those of NMQ with the shape parameter ϵ. We use the leave-one-out cross validation (LOOCV) algorithm [14] to find a suitable shape parameter ϵ for MQ. Direct KANSA and New KANSA respectively represent the results obtained by using the Kansa method directly and by the new formulation employed in this paper in the global case. Direct LKANSA and New LKANSA respectively represent the corresponding results for the local case. Direct MAPS, New MAPS, Direct LMAPS, and New LMAPS are defined similarly for the method of approximate particular solutions both in global and local cases.

To validate the numerical accuracy, we calculate the following root mean square error (RMSE),

$$RMSE = \sqrt{\frac{1}{q}\sum_{j=1}^{q}(\hat{u}_j - u_j)},$$

where q is the number of testing nodes chosen randomly in the domain, u_j and $\hat{u}_j$ denote the exact solution and approximate solution at the jth node, respectively. In the numerical results, n_i and n_b respectively represent the number of interior and boundary points.

Example 5.1. We consider the following partial differential equation with mixed boundary conditions:

$$(5.1) \qquad Lu(x,y) = f(x,y), \quad (x,y) \in \Omega,$$
$$u(x,y) = \sin(\pi x)\cosh(y) - \cos(\pi x)\sinh(y), \quad (x,y) \in \partial\Omega,$$
$$\frac{\partial u(x,y)}{\partial \mathbf{n}} = g(x,y), \quad (x,y) \in \partial\Omega,$$

where

$$L = \Delta^2 + x^2 y^3 + y\cos(y)\frac{\partial}{\partial x} + \sinh(x)\frac{\partial}{\partial y},$$

and $\mathbf{n}$ is the unit normal vector. $f(x, y)$ and $g(x, y)$ are generated from the analytical solution:

$$u(x, y) = \sin(\pi x)\cosh(y) - \cos(\pi x)\sinh(y).$$

The computational domain Ω as shown in Figure 1 is bounded by the curve defined by the parametric equation:

$$\partial\Omega = \{(x, y)|x = \rho\cos\theta, y = \rho\sin\theta, 0 \le \theta \le 2\pi\},$$

where

$$\rho = e^{\sin\theta}\sin^2(2\theta) + e^{\cos\theta}cos^2(2\theta).$$

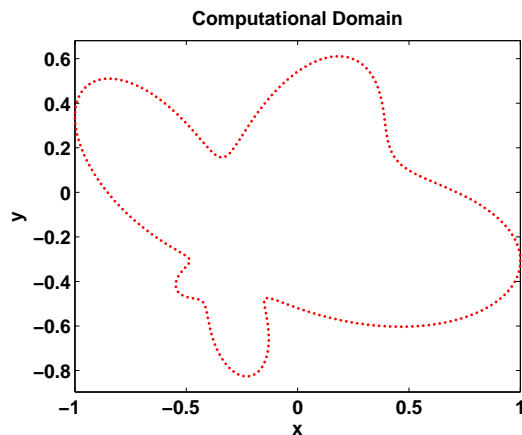FIGURE 1. Amoeba-shape Domain

TABLE 1. RMSE for New LMAPS and Direct LMAPS

(n_i, n_b)	New LMAPS			Direct LMAPS		
	RMSE	CPU Time	ϵ	RMSE	CPU Time	ϵ
(3809,500)	2.330e-03	5.95	1.52	9.030e-03	4.19	1.62
(15254,500)	2.630e-05	25.29	1.87	4.950e-03	15.40	1.65
(23850,500)	9.510e-06	40.13	2.54	2.770e-02	23.82	3.10

We list in Table 1 the numerical results for the LMAPS with Ω being an amoeba-shape domain. Numerical accuracy between New LMAPS and Direct LMAPS is almost the same for a small number of interior nodes. However, as the number of interior nodes increases, the New LMAPS is far more accurate than the direct one. Due to the large size of the matrix in the new formulation, the computational cost of the New LMAPS is slightly higher than that of the Direct LMAPS, which seems reasonable. The number of interior points is taken up to $23,850$ with 500 boundary points with an accuracy of 9.510×10^{-6} which is promising. We choose 21 nodes in the local domain. The stability of the normalized MQ as depicted in Figure 2 enables

us to find the stable solution in the New LMAPS by LOOCV. We observe the same kind of stability behavior in the Direct LMAPS as shown in Figure 3.
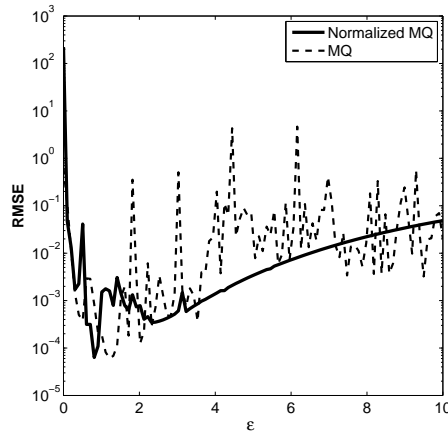

FIGURE 2. MQ versus NMQ in New LMAPS

TABLE 2. RMSE for New LKANSA and Direct LKANSA using NMQ

(n_i, n_b)	New LKANSA		Direct LKANSA	
	RMSE	ϵ	RMSE	ϵ
(3809,500)	3.673e-01	3.72	4.269e-02	2.36
(15254,500)	4.451e-04	4.67	1.227e-02	2.31
(23850,500)	6.311e-04	5.74	3.438e-02	3.11

We compare the numerical accuracy of the new local Kansa method with that of the direct local Kansa method in Table 2 with the same number of computational nodes as in Table 1. From the numerical results, we can easily observe that the new approach performs better than the direct one. Moreover, in this paper we want to compare the performance of NMQ over MQ. From Figures 2 and 3, we observe that NMQ has more stable results as compared with the results obtained from MQ.

TABLE 3. RMSE for New MAPS and Direct MAPS using NMQ

(n_i, n_b)	New MAPS		Direct MAPS	
	ϵ	RMSE	ϵ	RMSE
(60,30)	0.40	4.277e-04	0.35	1.361e-03
(126,60)	0.61	1.089e-04	0.71	5.600e-04
(208,90)	0.91	3.696e-05	1.41	1.665e-04
(507,180)	1.72	4.204e-05	2.47	1.056e-04

Tables 3 and 4 show the numerical results for the global RBF collocation methods such as Kansa method and MAPS. We compare the numerical accuracy between the

new formulation and direct ones. We test $60, 126, 208,$ and 507 different interior points for the amoeba-shape domain. When we increase the number of computational nodes, the new formulation performs better than the direct ones in both cases. In this case, we use 507 interior points, 180 boundary points, and 300 test points. The new MAPS has accuracy of 4.204×10^{-5} at shape parameter 1.72 and the new Kansa method has accuracy of 4.050×10^{-5} at shape parameter 1.32 which is at least one order of accuracy better than the corresponding direct ones for 507 interior nodes and 180 boundary nodes. From this observation, we can easily say that this new approach is equally suitable for global collocation methods also.
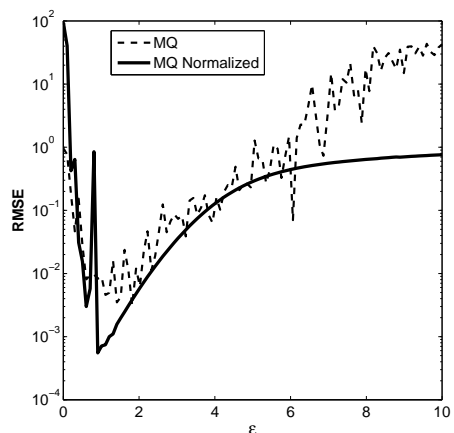

FIGURE 3. MQ versus NMQ in Direct LMAPS

TABLE 4. RMSE for New KANSA and Direct KANSA using NMQ

	New KANSA		Direct KANSA	
(n_i, n_b)	ϵ	RMSE	ϵ	RMSE
(60,30)	0.30	1.666e-04	0.71	2.304e-02
(126,60)	0.56	1.752e-04	0.91	1.583e-03
(208,90)	0.81	9.363e-05	1.01	2.411e-04
(507,180)	1.36	4.050e-05	1.01	1.474e-04

Example 5.2. We consider the following fourth-order partial differential equation:

$$(5.2) \qquad \begin{aligned} Lu(x,y) &= f(x,y), \ \ (x,y) \in \Omega, \\ u(x,y) &= y\sin(x) + x\cos(y), \ \ (x,y) \in \partial\Omega, \\ \Delta u(x,y) &= g(x,y), \ \ (x,y) \in \partial\Omega, \end{aligned}$$

where

$$L = \Delta^2 + xy + 2y\sin(x)\frac{\partial}{\partial x} - y\cos(x)\frac{\partial}{\partial y},$$

$f(x, y)$ and $g(x, y)$ are generated from the analytical solution:

$$u(x, y) = y \sin(x) + x \cos(y).$$

The computational domain is bounded by the following peanut-shape parametric curve as shown in Figure 4 :

$$\partial \Omega = \{(x, y)|x = \rho \cos \theta, y = \rho \sin \theta, 0 \le \theta \le 2\pi\},$$

where

$$\rho = \cos(2\theta) + \sqrt{1.1 - \sin^2(2\theta)}.$$
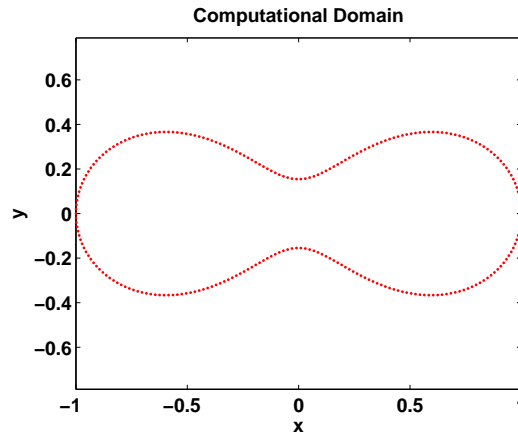
FIGURE 4. Peanut-shape Domain

In Tables 5 and 6, we compare the numerical results of global RBF collocation methods. In this example, we test fewer computational nodes as compared with the previous example. For the Kansa method, using only 293 interior points and 120 boundary points, the accuracy for the new Kansa method is 3.059×10^{-7}. Similar accuracy is obtained for the new MAPS with the same number of computational nodes. Due to the smooth boundary of the peanut-shape domain, the accuracy shows an improvement compared with the amoeba-shape domain which we can observe from the numerical results. In this example also, we observe that the new method performs at least one order of accuracy better than the direct ones. Moreover, from the result, we see that the accuracy improves quickly as the number of interior and boundary nodes increases.

The numerical results of the fourth-order convection-diffusion equation for local Kansa method and local MAPS are listed in Tables 7 and 8, respectively. In this example we use 15 points in the local subdomain. To solve this Dirichlet problem, we use different numbers of interior and boundary nodes for the normalized MQ. Here we observe that for only 1602 interior points and 80 boundary points, the accuracy for the new local Kansa method and direct local Kansa method are 1.761×10^{-6} and 4.584×10^{-4}, respectively, which are considerably good. As we increase the numbers

TABLE 5. RMSE for New KANSA and Direct KANSA using NMQ

(n_i, n_b)	New KANSA		Direct KANSA	
	ϵ	RMSE	ϵ	RMSE
(25,20)	0.20	2.204e-06	0.22	4.656e-04
(145,60)	0.07	2.552e-07	0.36	8.398e-06
(293,120)	0.12	3.059e-07	0.37	8.111e-06

TABLE 6. RMSE for New MAPS and Direct MAPS using NMQ

(n_i, n_b)	New MAPS		Direct MAPS	
	ϵ	RMSE	ϵ	RMSE
(25,20)	0.25	3.394e-06	0.20	5.315e-05
(145,60)	1.01	2.541e-07	0.43	7.622e-06
(293,120)	1.62	2.047e-07	0.86	6.248e-06

of the interior and boundary nodes the accuracy reaches 2.144×10^{-7} for the new local Kansa method, which is even better than the new LMAPS. From this numerical result we assert that the new approach is equally applicable for (5.2).

TABLE 7. RMSE for New LKANSA and Direct LKANSA using NMQ

(n_i, n_b)	New LKANSA		Direct LKANSA	
	ϵ	RMSE	ϵ	RMSE
(1602,80)	1.11	1.761e-06	0.51	4.584e-04
(2024,120)	0.91	1.010e-06	0.40	1.841e-04
(2508,180)	1.01	2.144e-07	0.35	1.039e-04

TABLE 8. RMSE for New LMAPS and Direct LMAPS using NMQ

(n_i, n_b)	New LMAPS		Direct LMAPS	
	ϵ	RMSE	ϵ	RMSE
(1602,80)	1.31	1.896e-06	0.66	1.088e-04
(2024,120)	1.62	1.059e-06	0.71	4.083e-05
(2508,180)	1.62	8.752e-07	0.10	5.458e-05

6. CONCLUSION

Solving fourth-order PDEs with high accuracy and efficiency is not an easy task. By using an intermediate step to reduce fourth-order PDEs to second-order PDEs,

we successfully implemented the new approach to solve various fourth-order PDEs. Numerical results show that the new formulation of RBF collocation methods outperformed the direct RBF collocation methods in both global and local cases. Here, we would like to emphasize the fact that the matrix size in the new formulation is twice that of the direct formulation, however, it is still efficient and accurate. From the numerical results, we observe that the new formulation has at least one order of accuracy better than the direct ones. Moreover, the use of the normalized MQ seems to have very stable results compared to the results obtained by MQ. LOOCV is able to catch the optimal shape parameter due to the stability of the normalized MQ even in the local case.

ACKNOWLEDGMENTS

REFERENCES

[1] Buhman MD. Radial basis functions, theory and implementations. Cambridge University Press, 2003.

[2] Chen CS, Fan CM, Wen PH. The method of approximate particular solutions for solving elliptic problems with variable coefficients, Int J Comput Methods 8(3): 545–59, 2011.

[3] Chen CS, Ganesh M, Golberg MA, Cheng AHD. Multilevel compact radial basis functions based computational scheme for some elliptic problems. Comput Math Appl, 43:359–78, 2002.

[4] Chen W, Fu ZJ, Chen CS. Recent advances in radial basis function collocation methods, Springer, 2013.

[5] Cheng, AHD. Particular solutions of Laplacian, Helmholtz-type, and polyharmonic operators involving higher order radial basis functions. Eng. Analy. Boundary Elements,24:531–538, 2000.

[6] Halpern D, Jensen OE, Grotberg JB. A theoretical study of surfactant and liquid delivery into the lung, Journal Appl. Physiology, 85:333–352, 1998.

[7] Kansa EJ. Multiquadrics - a scattered data approximation scheme with applications to computational fluid dynamics-ii. Comput Math Appl, 19:147–161, 1990.

[8] Kim S, Lim H. Fourth-order PDEs for effective image denoising. Electronic Journal of Differential Equations, 107–121, conf 7, 2009.

[9] Lamichhane, AR, Chen CS. Particular solutions of Laplace and bi-harmonic operators using Matern radial basis function. Int J of Compu Math. DOI: 10.1080/00207160.2015.1127359

[10] Lysaker M, Laudervold A, Tai XC. Noise removal using fourth-order PDE with applications to medical magnetic resonance images in space and time. IEEE Transanctions on Image Processing, Vol 12, No.12, Dec 2003.

[11] Mai-Duy N, Tran-Cong T. Mesh-free radial basis function network methods with domain decomposition for approximation of functions and numerical solution of Poisson's equation. Eng Anal Bound Elem, 26:133–156, 2002.

[12] Monroe, J. Hybrid meshless method for the numerical solution of PDEs. USM Dissertation, 2014.

[13] Myers TG, Charmin JPF, Chapman SJ. A mathematical model for atmospheric ice accretion and water flow on a cold surface. Int J Heat Mass Tran, 47:5483–5500, 2004.

[14] Rippa S. An algorithm for selecting a good value for the parameter c in radial basis function interpolation, Adv in Compu Math, 11:193–210, 1999.

[15] Sarler B, Vertnik R. Meshfree explicit local radial basis function collocation method for diffusion problems. Comput Math Appl., 51:1269–1282, 2006.

[16] Tsai CC, Cheng AHD, Chen CS. Particular solutions of splines and monomials for polyharmonic and products of helmholtz operators. Eng Anal with Bound Elem, 33:514–521, 2009

[17] Wendland H. Scatter data approximation. Cambridge University Press, Cambridge, 2005.

[18] Yao G, Chen CS, Kolibal J. A localized approach for the method of approximate particular solutions. Comput Math Appl, 61:2376–2387, 2011.

[19] Yao G, Tsai CH, Chen W. The comparison of three meshless methods using radial basis functions for solving fourth-order partial differential equations. Eng Anal Bound Elem, 35:600–609, 2011.